Renewable Energy 96 (2016) 341–353

Contents lists available at ScienceDirect

Renewable Energy

journal homepage: www.elsevier.com/locate/renene

Effects of bottom profile of an oscillating water column device on its hydrodynamic characteristics

S. John Ashlin, V. Sundar*, S.A. Sannasiraj

Department of Ocean Engg., Indian Institute of Technology Madras, India

ARTICLE INFO

Article history:
Received 11 July 2015
Received in revised form
11 April 2016
Accepted 29 April 2016
Available online 7 May 2016

Keywords:
Oscillating water column
Optimum air damping
Bottom profile optimization
Hydrodynamic efficiency
Wave amplification
Pressure ratio

ABSTRACT

The oscillating water column, OWC device is one of the more promising devices for the extraction of energy from ocean waves. The present study mainly focuses on the influence of bottom profile configuration in the OWC on its hydrodynamic performance. Four different bottom profiles flat, circular curve of radius 300 mm, slope of 1:1 and 1:5 were tested in a wave flume. The said models were simultaneously subjected to both regular and random waves. The hydrodynamic performance was studied in terms of wave amplification factor, wave power absorption coefficient, hydrodynamic efficiency, lip wall pressure ratio (pressure at in front of lip wall/pressure due to incident wave) and air pressure ratio (air pressure/pressure due to incident wave). It is found that the natural period of the system was around 1.9 s. The OWC with circular curve bottom profile exhibited a better performance in terms of its effective wave energy conversion and wave amplification factor inside the chamber. The peak magnitude of hydrodynamic efficiency for circular curve bottom profile was 0.71. The performance of the OWC model is found to be better when closer to the natural period of the device.

1. Introduction

Among the renewable energy resources, ocean energy is the one, which is available in abundance around the globe. Ocean energy is available in the forms of ocean thermal energy (direct effect of solar radiation on the sea), wave energy (result of balancing nature between gravitational and wind force), tidal energy (due to the attraction between celestial bodies), ocean currents (due to the gradient of salinity, temperature, etc.), etc. The energy in the ocean waves is due to the imbalance between gravitational force and shear due to wind. It travels thousands of kilometers as a Swell wave without any energy loss from the place where the energy is imparted on the water surface. As the waves travel from deep to shallower water region, certain amount of energy (potential energy + kinetic energy) dissipates, particularly in the breaking zone. The level of dissipation as well as an increase in its amount depends on several parameters, of which the most important are seabed friction, bathymetry, and presence of obstructions. Nevertheless, the wave power available in the near shore is quite enough to produce electricity as it is directly proportional to the square of the amplitude of the wave and its wavelength.

Since the past several years, scientists and engineers have been working in the field for an effective device to extract the ocean wave energy. Wave energy convertors, WECs have been installed in countries like UK, USA, Norway, India and Japan. Considerable amount of literature on this topic have been reported by McCormick, Shaw and Ross [8,12,14]. Wave energy convertors (WEC), can be classified as per location, working principle as follows [1]:

(i) Based on its distance from coast as on-shore (less than 8 m in which case it facilitates integration with detached offshore breakwaters serving as coastal protection hard structure), near-shore (devices installed in depths between 8 and 20 m), and offshore devices (built in water depths greater than 20 m).
(ii) Based on its principle of operation, may be classified as point absorber buoy, surface attenuator, terminator, oscillating water column and overtopping devices.

Among the different types of WECs, the Oscillating Water Column (OWC) is claimed to be simple in its concept which has been installed and tested in a number of fields. A 125 kW OWC bottom-standing power plant situated in Kerala along the west coast of India [10] and a 75 kW LIMPET OWC power plant off the Island of

* Corresponding author.
E-mail address: vsundar@iitm.ac.in (V. Sundar).

http://dx.doi.org/10.1016/j.renene.2016.04.091
0960-1481/

Islay, Scotland, UK [19] are a few important standing examples. Further, the 75 kW LIMPET was decommissioned in 1999 and led to the construction of a larger rated device of 500 kW in 2000. A summary of OWC's around the globe has been reported by Sundar et al. [13]. The OWC consists of a chamber with a partially submerged front wall that is continuously excited by the ocean waves. Due to wave excitation, during the instant of its crest inside the chamber the air column is compressed, whereas, the presence of its trough expands the air column. This leads to oscillation of air column and thus, the system acts like a pump which could be easily converted into meaning energy by driving a turbine on board the OWC. The turbine should be capable of rotating in the same direction irrespective of the reversible flow inside the chamber due to the passage of crest and trough. Wells turbine, is the most popular one handling this requirement with higher degree of efficiency. Since several decades, researchers have been involved in the improvement of the performance efficiency of OWC mostly tuning its configuration with respect to the wave climate.

It was inferred by Malmo and Reitan [7] that the natural frequency of an OWC system primarily depends on its front lip depth. McIver and Evans [9] observed that the reaction of OWC system depends on the extent of the dynamic pressure and its excitation period, whereas, Zheng et al. [22] proved that flared harbor walls in an OWC enhanced its efficiency compared to the one with rectangular walls. Evans and Porter [2] considered the air chamber length (b), water depth (d) and the submergence of lip wall (s) to be the main parameters dictating the efficiency of an OWC. It was inferred that for lower values of the ratio, b/d, and the behavior of fluid like a rigid body inside the OWC air chamber. It was also reported that for higher values of s/d, the frequency band of efficiency was becoming narrow. In this study, the thickness of lip wall is not considered. Through a detailed experimental study on OWC, Thiruvenkatasamy and Neelamani [15] found that an increase in wave steepness causes a decrease in its performance in terms of its efficiency and for a/A (ratio of air hole area (a) to plan area (A)) larger than 0.81%, a considerable reduction in energy absorption capability of the device was reported. Tseng et al. [17] reported that the experimental investigation on multi-resonant oscillating water column yields only 28.5% of efficiency because of high-energy loss. Wang et al. [18] studied analytically and experimentally the change in bottom slope in front of the shoreline mounted OWC model and observed that an increase in the slope of the bottom leads to a shift in the capture-width ratio at lower frequencies. The capture width is defined as the ratio of averaged output power from the system to the input power offered by waves. The thickness of the front wall did not have any influence on energy conversion capacity of the device as is claimed by Thomas et al. [16] through an experimental study. It was stated by Folley et al. [4] that the potential of near shore exploitable wave energy source is as similar to offshore sites. Zhang et al. [21] observed that the efficiency of OWC centered on a resonant frequency. This clearly shows the importance of phase lag between the dynamic excitation pressure and the corresponding air pressure being developed. Wilbert et al. [20] have considered the parameters such as water depth inside the wave energy converter (d) and opening at its base (o) and reported that effective energy conversion capacity of OWC was found to be increasing with an increase in its bottom opening, o/d. It reached a maximum efficiency of 94% closer to the natural frequency for o/d = 0.80. However, at the same time, the peak efficiency was found to shift towards the higher frequency with an increase in opening depth. Rezanejad et al [11] studied about change in stepped sea bottom effects on the efficiency of the OWC device based on the two dimensional linear water wave theory. It was reported that introducing step outside the chamber have significant effects on increasing its efficiency.

Sundar et al. [13] presented a comprehensive review on the possible approaches of integrating OWC with breakwaters for the harbor formation and coastal defense systems. The concept of integration of OWC with breakwaters that can reduce the total cost significantly to bring forth economic security in project planning was highlighted. Even though there have been considerable studies on optimizing OWC, the effect of bottom profile inside the chamber on its efficiency is an area that is yet to be explored. Hence, in the present study, an attempt is made to understand the effect of the bottom profile of the OWC on its efficiency which could be integrated with breakwaters. The idea of this study is to replicate such a condition in the laboratory, and hence, the OWC models were subjected to wave action without side clearance or otherwise not allowing waves to pass around the structure. The details of the OWC models, experimental set-up, wave characteristics, experimental procedure, results and discussion are reported in this paper.

2. Dimensions of the OWC

In the design of OWC, there is a hidden assumption that its performance mainly depends on the pressure excitation and natural frequency of the chamber. According to this, the dimensions are fixed to harness maximum efficiency. The key parameters of OWC is the depth of its front lip wall immersed in to the water, length, width of the chamber and optimum air damping to the system. According to Thomas et al. [16] a decrease in the bottom opening 'o', (increasing lip wall depth) reduces the natural frequency of the OWC leading to its ineffectiveness in absorbing energy, in which case, the bandwidth of the efficiency peak becoming narrower and thus decreasing the effective area under the efficiency curve. Wilbert et al. [20] reported the efficiency of an OWC increases with an increase in the bottom opening. For the considered o/d of 0.15, 0.30, 0.45 and 0.80 observed that a higher efficiency for o/d of 0.80. Since, the waves in nature are random, larger bottom opening can result in the trough propagating much below the tip of the lip wall leading to the penetration of air into the OWC chamber that would cause stalling of the turbine. To avoid such a precarious situation, in the present study the ratio of bottom opening to the water depth (o/d) is fixed as 0.6. The claim of Thomas et al. [16] that the bottom edge of the front lip wall of the OWC instead being sharp if curved leads to an increase in its efficiency was also incorporated in the models considered in this study. Wilbert et al. [20] through laboratory studies, suggested that the ratio of the length of the chamber (b) to the design wave length (L), (b/L) should be in between 0.09 and 0.1. If the predominant wave period along the coast is known to harness maximum wave energy, the length of OWC 'b' (along the wave direction) could be fixed. As the present study, considers a wave period ranges from 0.8 s to 3.0 s that correspond to 'L' ranging between 1 m and 6.5 m, 'b' was fixed as 0.3 m. The efficiency of the OWC also depends on the optimum air damping represented by ratio of area of the air hole in the air chamber in the OWC, a to the plan area of the air chamber, A.

3. Experimental setup

The experimental investigation was carried out in a wave flume of 72.5 m long, 2 m wide and 2.5 m deep in Indian Institute of Technology Madras, India. Four different 1:12 scale devices of OWC's (characterized by four different bottom profiles: flat bottom, circular curve bottom of radius 300 mm, bottom with a slope of 1:1 and 1:5)) were subjected to wave action. For simultaneous testing of these four OWC models and to avoid the phenomena of interaction due to radiation waves, the flume was divided into four equivalent parts and dividers extended 15 m from each of the

model towards the wave maker direction. Consequently this leads to fixing the width of the OWC 'w' (perpendicular to the wave direction) as 0.471 m. OWC devices were made-up of acrylic sheets of 12 mm thickness. An inner dimension of an air chamber was 0.471 m × 0.3 m and the height of the model was about 0.9 m with a front lip wall of 0.6 m depth and 0.3 m water inlet to a chamber from the bottom of a chamber. The water depth in the flume, d was maintained at 0.5 m. The wave flume is equipped with a wave maker capable of operating in hinged and piston mode in order to generate both deep and shallow water waves. A beach on the other end in the shape of parabolic and perforated in nature is able of absorbing energy from the waves about 90%. The OWC devices were rigidly fixed at 45 m away from the wave maker. The test duration and the model placing position in the wave flume have been chosen in such a way to avoid re-reflection from the wave maker without the need of using active wave absorption system. The analysis for the measurements were carefully done in the steady state region. The longitudinal and plan view of the present experimental setup with marking of cross section for different bottom profile is shown in Fig. 1. The dimensional details of the different bottom profile OWC models corresponds to the cross sectional elevation are shown in Fig. 2. A view of the OWC units with four different bottom profiles in the wave flume is projected in Fig. 3. The regular wave tests, the wave characteristics covered wave steepness (H/L) ranging from 0.0122 to 0.0515 with relative water depth (d/L) from 0.0993 to 0.3302. Similarly, the random wave tests, covered wave steepness, H_{m0}/L_p defined as the ratio of spectral estimate of significant wave height, H_{m0} to the wavelength corresponding peak wave period, L_p varying from 0.0141 to 0.0564 with d/L_p ranging between 0.0782 and 0.3307. The spectral width parameter, ε for the tests varied between 0.5 and 0.75. For the random waves defined by the two parameter Pierson Moskowitz (PM) spectrum was employed which is as given as,

$$S(f) = \frac{5H_s^2}{16 f_p}\left(\frac{f_p}{f}\right)^5 \exp\left[-\frac{5}{4}\left(\frac{f_p}{f}\right)^4\right]. \quad (1)$$

Three number of resistance type wave probes, one at 7 m from the wave maker for registering the incident wave elevation, η_1 (t) and the other two at 5 m, η_2 (t) and 5.31 m, η_3 (t) from the model, inside each of the four longitudinal sections, were used to determine reflection coefficient as per the method of Goda and Suzuki [5]. In addition, the run-up (R_u(t)) due to water surface oscillations on the rear wall of the OWC chamber was measured. Two pressure transducers with a measuring range of 0.2 bar one front wall outside pressure at mouth of the OWC chamber facing the waves (p_{fout}(t)) and another fixed on its inner side (p_{fin}(t)) registered the respective pressure time histories for each of four OWC models. The air pressure variation due to rise and fall of free surface water inside the chamber of each of the four models was measured with a pressure sensor fixed on top (p_{air}(t)) of the OWC models. All the signals were acquired simultaneously with a sampling interval of 0.05 s. The initial tests with OWC models of flat bottom with a/A varying between 0.1 and 1.2% in steps of 0.1% were performed with regular waves in order to assess the area of the opening for higher efficiency.

4. Hydrodynamic parameters

The different hydrodynamic parameters that were considered under the study to evaluate hydrodynamic performance of the structure are as defined below. The hydrodynamic efficiency of an OWC device in regular waves, λ_{reg} is calculated by the ratio between pneumatic output power to the incident wave power flux as follows,

$$\lambda_{reg} = \frac{P_{out}}{P_{in}} \quad (2)$$

The incident wave power flux (P_{in}) as a function of wave height (H), wave period (T), water depth (d) and width (w) is given as,

$$P_{in} = \frac{\rho g H^2}{8}\frac{C}{2}\left(1 + \frac{2kd}{\sinh 2kd}\right)w \quad (3)$$

whereas, C = L/T, k = 2π/L and L = wave length.

Due to rise and fall of water inside the chamber, the pneumatic output power (P_{out}) being developed is calculated by instantaneous integration of free surface oscillation inside the chamber moving with velocity (V_w) under the air pressure (p_{air}) as follows,

$$P_{out} = \frac{1}{T}\int_t^{t+T} p_{air} A V_w dt \quad (4)$$

herein, V_w is the first derivative of the third-order approximation to the free surface elevation inside the chamber [6] calculated by the expression as,

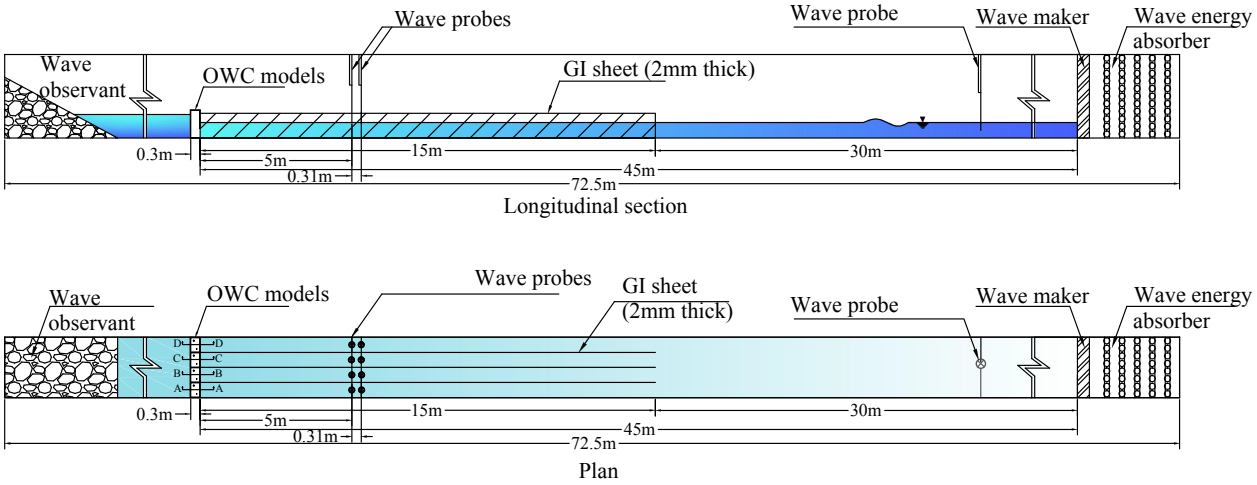

Fig. 1. Test set-up.

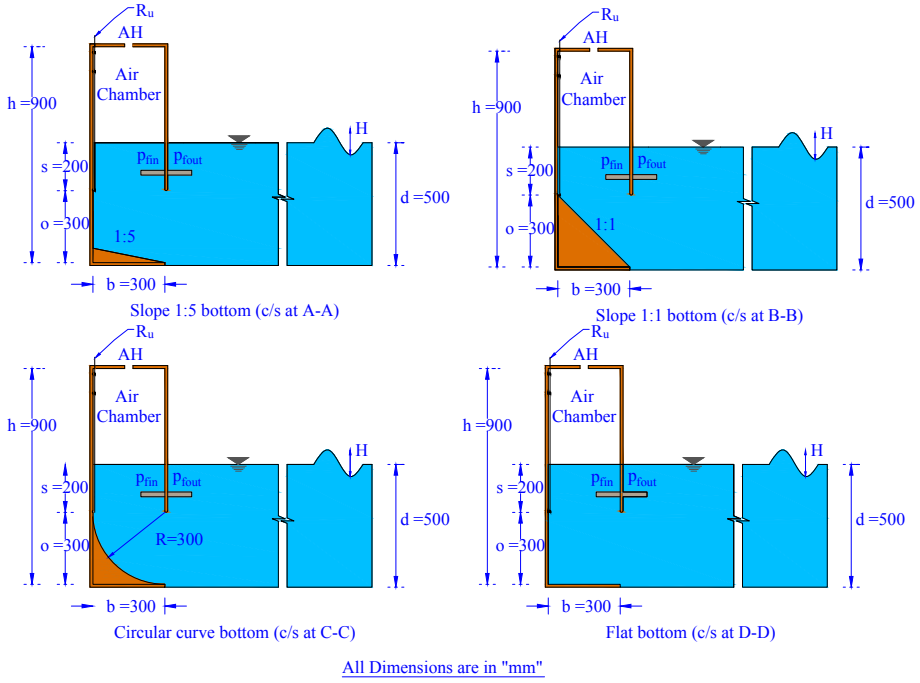

Fig. 2. Cross sectional details of OWC.

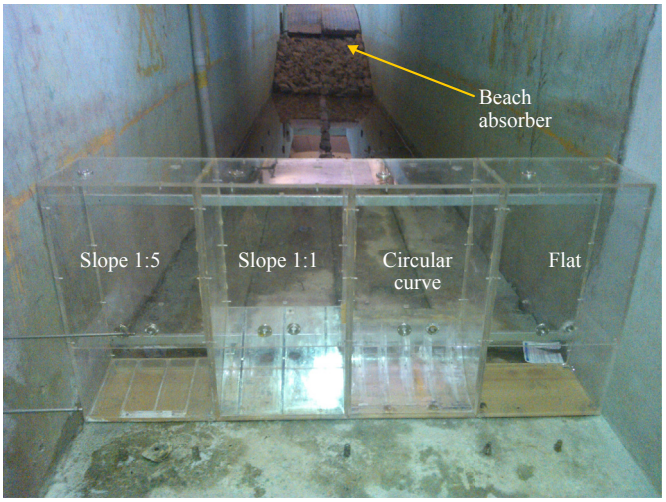

Fig. 3. Four different bottom profiles of OWC.

$$V_w = \frac{2z_{i+1} + 3z_i - 6z_{i-1} + z_{i-2}}{6\Delta t} \tag{5}$$

where, z_i is the elevation of free surface at time t_i and Δt is the sampling interval. The hydrodynamic efficiency for the OWC in random wave field, λ_{ran} is expressed as,

$$\lambda_{ran} = \frac{P_{out}}{P_{ave(in)}} \tag{6}$$

The average input power is calculated through the expression given below,

$$P_{ave(in)} = w\rho g \sum_{i=1}^{N} S_i (C_g)_i \Delta f \tag{7}$$

whereas, ρ = mass density of fluid, g = gravitational acceleration, N = number of frequency bands (each with a width of Δf), S_i = spectral density at ith band and $(C_g)_i$ = group velocity at ith band. The group velocity is given by,

$$(C_g)_i = n_i C_i \tag{8}$$

herein,

$$n_i = \frac{1}{2}\left(1 + \frac{2k_i d}{\sinh(2k_i d)}\right) \tag{9}$$

In order to quantify the pressure ratio in front of the lip wall of OWC, (PR_{fout}) and inside the air chamber, (PR_{air}) were calculated as ratio of $(p_{fout})_{max}$ and $(p_{air})_{max}$ (from crest to trough) to the incident wave pressure respectively. In the case of random waves, zeroth spectral moment of (p_{fout}) and (p_{air}) are considered. For both regular and random waves the expressions for calculating pressure ratios are given as follows,

$$\left(PR_{fout}\right)_{reg} = \frac{\left(p_{fout}\right)_{max}}{\rho g H} \tag{10}$$

$$\left(PR_{fout}\right)_{ran} = \frac{\left(p_{fout}\right)_{m0}}{\rho g H_{m0}} \tag{11}$$

$$(PR_{air})_{reg} = \frac{(p_{air})_{max}}{\rho g H} \tag{12}$$

$$(PR_{air})_{ran} = \frac{(p_{air})_{m0}}{\rho g H_{m0}} \quad (13)$$

whereas, $(p_{fout})_{m0}$ is the significant pressure registered in front of the OWC lip wall, $(p_{air})_{m0}$ is the significant pressure registered inside the air chamber and H_{m0} is the significant wave height.

The wave amplification factor, defined as the ratio of the free surface oscillation inside the OWC chamber, $(R_u)_{max}$ (from crest to trough) to the incident wave height for both regular and random waves are denoted as follows,

$$\beta_{reg} = \frac{(R_u)_{max}}{H} \quad (14)$$

$$\beta_{ran} = \frac{(R_u)_{m0}}{H_{m0}} \quad (15)$$

where, $(R_u)_{m0}$ is the significant water surface elevation measured inside the OWC chamber. The wave power absorption coefficient for the OWC device exposed to regular waves, WPA_{reg} is obtained as,

$$WPA_{reg} = \frac{P_{fin}}{P_{in}} \quad (16)$$

$$P_{fin} = \frac{1}{T}\int_{t}^{t+T} p_{fin} A V_w dt \quad (17)$$

herein, P_{fin} = Wave power available inside the chamber. For the random waves, the wave power absorption coefficient, WPA_{ran} is through the Eqn. (18) as given below,

$$WPA_{ran} = \frac{P_{fin}}{P_{ave(in)}} \quad (18)$$

Higher the value of wave power absorption coefficient indicates higher the fluid pressure absorbed at the mouth of the chamber.

5. Results and discussion

5.1. Time histories of measured parameters

Typical time histories of wave surface elevations (η_1, η_2 and η_3), pressure head in front of the lip wall (p_{fout}), inside the lip wall (p_{fin}), air pressure head (p_{air}) within OWC, and run-up, $R_u(t)$ measured in the compartment housing the OWC with the circular curve bottom subjected to random wave field characterized by $H_{m0} = 0.12$ m and $T_p = 2$ s along with their corresponding spectral plots are depicted in Fig. 4. It is observed that $p_{fout} > p_{fin} > p_{air}$ due to loss of energy because of reflection, vortices formation and radial flow of wave inside the chamber.

5.2. Optimization of air vent through tests

As one of most important parameter being the size of air vent, an effort has been to investigate its effect in terms of a/A on the efficiency of the OWC as an initial step. This is absolutely essential as once this aspect is frozen, a detailed investigation can then follow with the structural parameters including its bottom profile that can be tuned for the wave characteristics. For this purpose as stated earlier the a/A was varied from 0.1 to 1.2% in steps of 0.1%. The variation of hydrodynamic efficiency of the flat bottom OWC, λ_{reg} as a function of d/L for different a/A are superposed in Fig. 5a and b.

It is clearly seen that λ_{reg} increases with an increase in a/A up to 0.6% and thereafter a reverse trend in its variation is seen. For smaller a/A, air damping in the system will be higher and tend to suppress or attenuate the rise in the oscillating water column. The damping reduces with an increase in a/A up to an optimum a/A. If a/A increases, the compression due to oscillation of free surface water inside the air chamber decreases, phenomenally the pressure difference between inside the chamber and outside will be low which would lead to a decrease in the efficiency of the OWC. As the transition was observed to take when a/A is in between 0.6% and 0.7%, tests were conducted with an additional a/A of 0.68%, which is seen to yield a slightly higher λ_{reg}. It is to be mentioned that Thiruvenkatasamy and Neelamani [15] have claimed that the efficiency decreases if a/A more than 0.81%. However, an in-depth investigation into this aspect was not carried out by them. From the forgoing results, the a/A for all the four models considered herein was fixed as 0.68%.

5.3. Hydrodynamic efficiency

The hydrodynamic efficiency for the regular waves was found by the formulae given in Eqn. (2). For OWC models with different bottom profiles in a constant water depth as mentioned earlier, the variation of λ_{reg} with d/L for finite range of H/L for the tests with regular waves are shown in Fig. 6a–d.

The trend in the variations for all the models is found similar. The results show the λ_{reg} initially increases with an increase in d/L reaching a maximum value of about 0.71 at d/L = 0.131 which corresponds to the natural period of the OWC model of 1.9 s. In general, it is seen that the H/L has a significant influence on λ_{reg} to an extent of 25%–35% for low frequency waves, i.e., lower d/L. For d/L < 0.131, is seen that λ_{reg} is less for higher H/L, is due to the fact that a greater part of the incident wave energy gets reflected and hence reduces the energy available for driving the air column. This is evident from the plots on the variations of reflection coefficient, $k_{r(reg)}$ for the models that are discussed later. For d/L > 0.15, the influence of H/L is found to be less. Higher the waves, there could be a possibility that the trough of the wave may tend become deeper and propagate below the front lip wall, in which case, the pressure within the chamber walls be equivalent to atmospheric pressure for a considerable duration. Under such a situation, the power available inside the OWC is zero causes a decrease in its efficiency, which needs to be kept in mind while designing OWC for a prevailing wave climate. Furthermore, as the λ_{reg} is found to be maximum for the lowest range of H/L = 0.0122 to 0.0194, only for this range, the variation of λ_{reg} for the four models are superposed in Fig. 7. As stated earlier due to higher reflection from the lip wall as well from the inner wall of the OWC model with bottom profile of slope 1:1 the λ_{reg} found to be less compared to the other three.

In order to examine the effect of wave length on circular curve bottom profile OWC on its efficiency the time series quantifying phase difference between $(PR_{fout})_{reg}$, β_{reg}, $(PR_{air})_{reg}$ against t/T is shown in Fig. 8 for a constant H of 0.055 m. It is seen that the pressure ratio measured in front of the lip wall of OWC and wave amplification factor increases with a decrease in d/L or increase in L. At the same time, the air pressure ratio inside the chamber increases with an increase in wave length up to the natural period of the device (d/L = 0.131) beyond which, $(PR_{air})_{reg}$ reduces. Higher the d/L implies smaller orbital motion, in which case, interference of the lip wall of OWC would be significant leading to vortex formation on its leeside. This will result in a breakdown of the motion of the free surface inside the chamber which results in lower water surface elevation (R_u) and hence reduced efficiency. The phenomena causing reduction in efficiency beyond the natural period of the device explained by quantitative measurement of phase difference

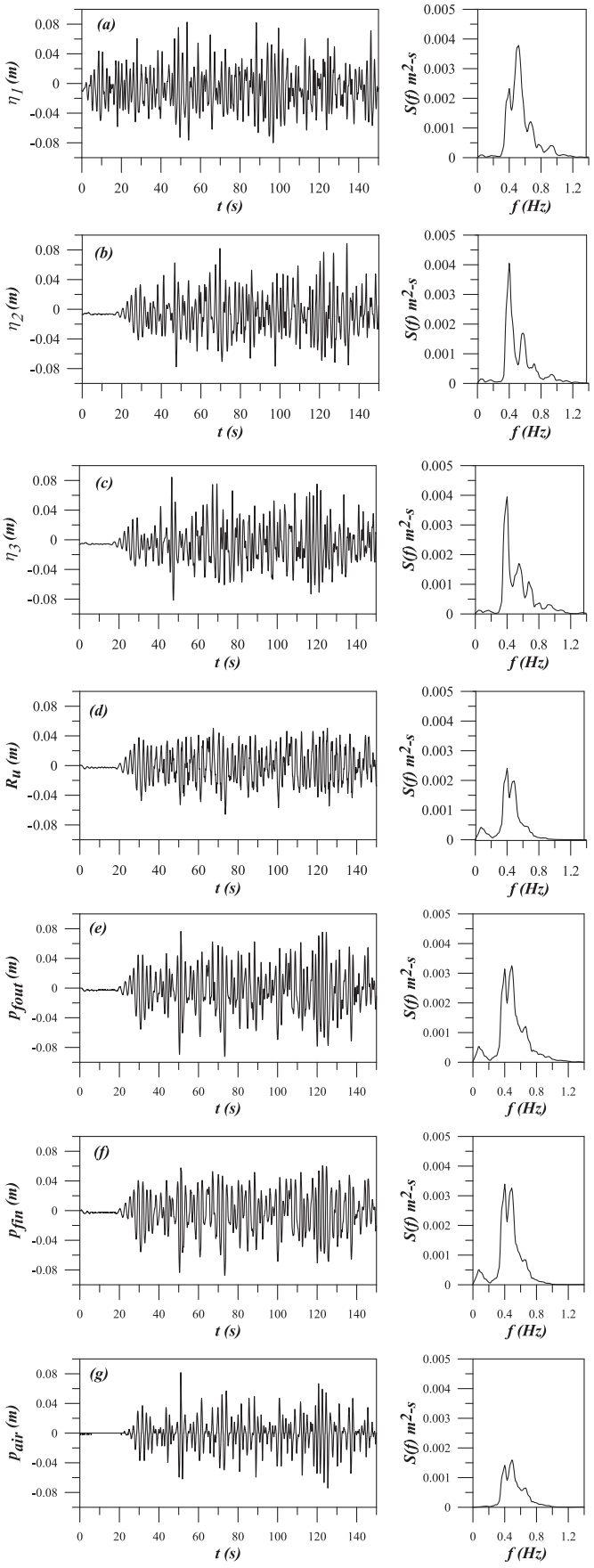

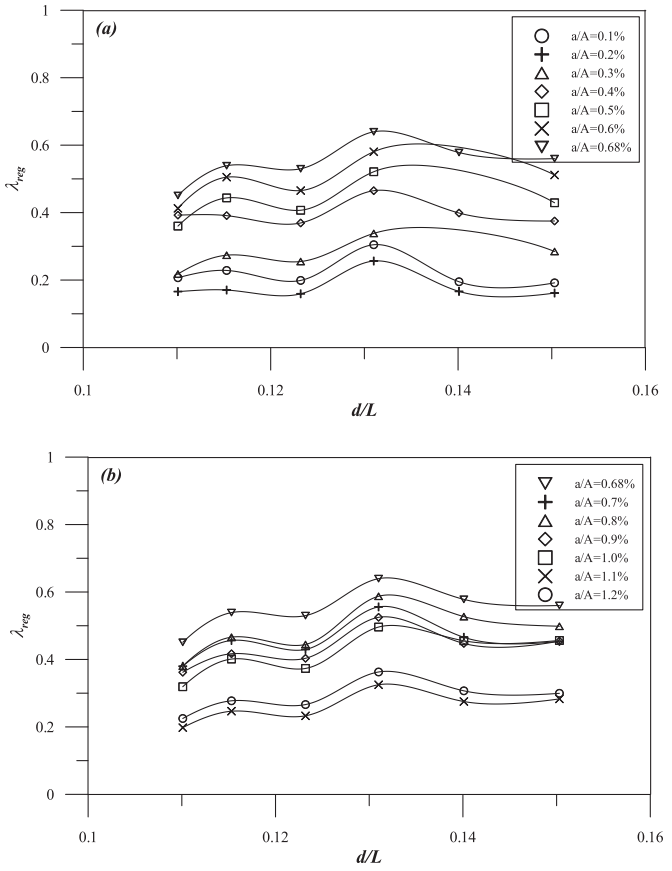

Fig. 5. Hydrodynamic efficiency (λ_{reg}) Vs d/L for different air damping ratios. (a) a/A from 0.1% to 0.68%, (b) a/A from 0.68% to 1.2%.

between hydrodynamic parameters $(PR_{fout})_{reg}$, β_{reg} and $(PR_{air})_{reg}$. The phase difference between these three parameters from the above results as a function of t/T is reported in Table 1, from which it is clearly seen that the phase difference between β_{reg} and $(PR_{air})_{reg}$ is large for higher frequency waves. Further, the phase difference decays towards the natural period of the system (d/L = 0.131) and beyond which it increases. From Eqn. (4) the output power of the system is instantaneous integration of air pressure and flow, which infers higher the phase difference reduces the efficiency and vice versa. This is the reason behind the reduction of efficiency of the system beyond the natural period of the device even though the β_{reg} increases due to an increase in the wave length. The detailed discussion on variation of $(PR_{fout})_{reg}$, β_{reg}, $(PR_{air})_{reg}$ corresponds to different d/L are discussed later.

The energy modulation effect due to the bottom profile of OWC due to random waves is quantified in Fig. 9a–d.

The trend in the variation of λ_{ran} with d/L_p (L_p is the wave length corresponding to T_p) for the four different models is found to be almost similar to that observed for the regular waves. However, the effect of wave steepness is found significant over the entire range of d/L_p. This significant variation in λ for random waves is due to the complex and random in nature of interaction between entry and exit of air pressure from the air chamber as well as the secondary flow that causes radiated flow inside the chamber. The variations of λ_{ran} with d/L_p for the lowest range of H_{m0}/L_p (0.0141–0.0199) for

Fig. 4. Time histories of (a) η_1, (b) η_2, (c) η_3, (d) R_u, (e) p_{fout}, (f) p_{fin}, (g) p_{air} for the circular curve bottom OWC. (Significant wave height (H_{mo}) = 0.12 m, Peak wave period (T_p) = 2 s).

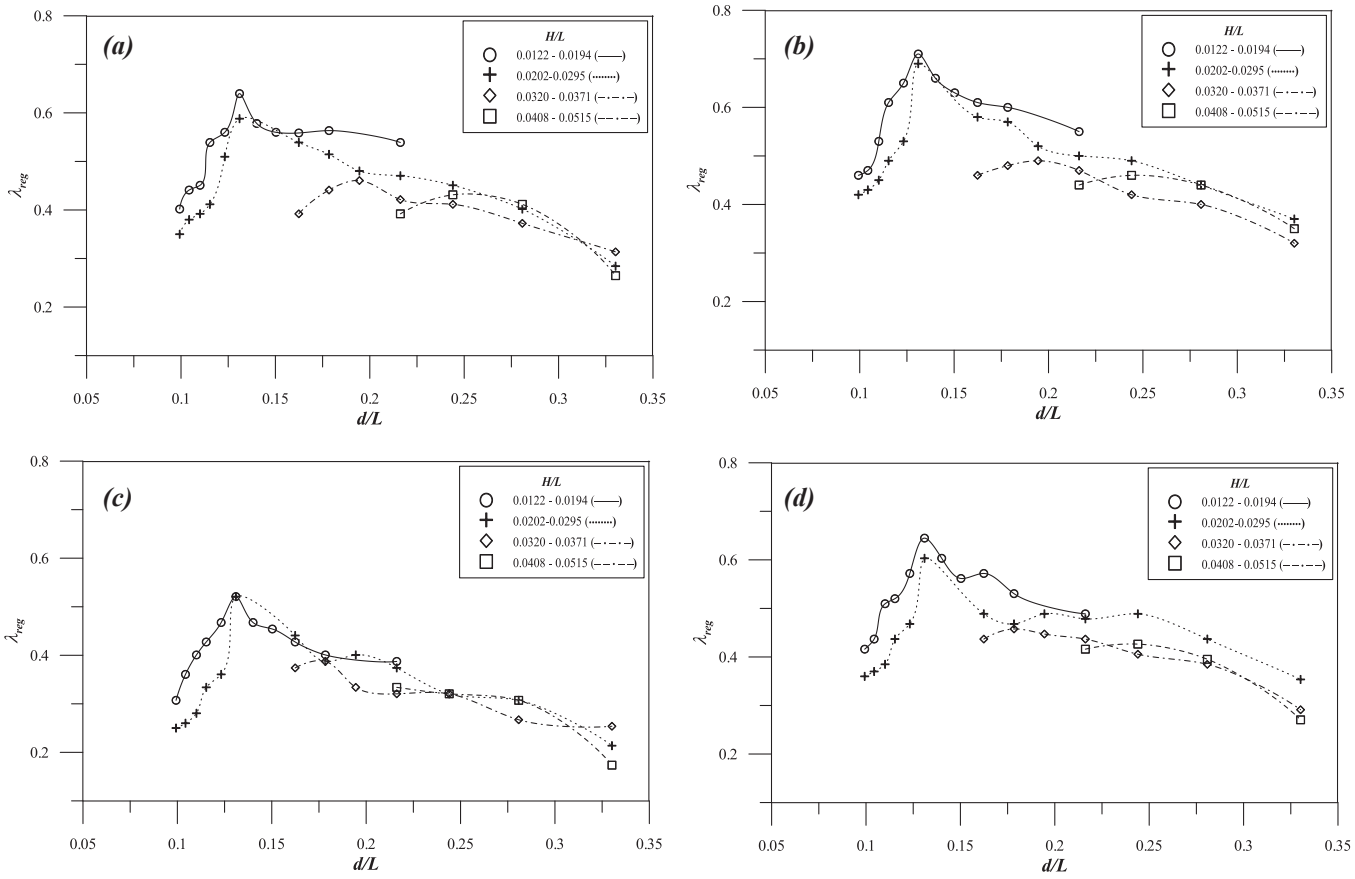

Fig. 6. a Hydrodynamic efficiency (λ_{reg}) of flat bottom OWC corresponds to the relative water depth. (Regular waves). b Hydrodynamic efficiency (λ_{reg}) of circular curve bottom OWC corresponds to the relative water depth. (Regular waves). c Hydrodynamic efficiency (λ_{reg}) of slope 1 in 1 bottom OWC corresponds to the relative water depth. (Regular waves). d Hydrodynamic efficiency (λ_{reg}) of slope 1 in 5 bottom OWC corresponds to the relative water depth. (Regular waves).

the four different models superposed in Fig. 10 show that the OWC with a curved bottom experiences maximum efficiency similar to the results we have seen for tests with regular waves. As the λ_{ran} is found to be a maximum for the lowest range of wave steepness for both the regular and random waves, only for this range, the variation of other parameters for the four models henceforth will be discussed.

5.4. Pressure ratio in front of the OWC chamber mouth

The variations of the dimensionless pressure on the seaside of the front wall due to regular waves, $(PR_{fout})_{reg}$ as well as random waves, $(PR_{fout})_{ran}$ based on the Eqns. (10) and (11) for the four models as a function of their respective relative water depths are projected in Figs. 11 and 12 respectively. The measurements of the said pressure are registered at close to the mouth of the OWC chamber. It is observed that the pressures for the model with flat and 1:1 slope experiences maximum pressures due to wave amplification in front of the chamber and higher reflection. It is found that the pressures are the least for the model with curved bottom with slightly higher for that with a bottom slope of 1:5. This is because of the smooth entrance offered to the propagation of the wave by which it is possible that most of the energy is absorbed by the OWC chamber. The pressures for all the models are found to exhibit a similar decreasing trend in their variation with an increase relative water depth as pressures due to long waves are higher. For d/L greater than 0.16, the variation in pressures for any of the models is not significant. Further the insignificant variation in pressures for d/L < 0.131 confirms, the optimum condition of the energy absorption of the wave energy device has reached. In the case of the results from random wave tests, a sudden drop in pressure at d/L_p of 0.1233 (L_p corresponds to the natural period of the system of 2 s) due to maximum energy absorbed by the chamber is clearly seen for all the models.

This confirms the criteria adopted for the selection of the dimensions of the wave energy convertor afore discussed. Further, around the natural frequency of the system, the effect due to the radiated flow will be less due to minimum phase difference between the incoming wave and water oscillation inside the chamber. Hence, from the above results due to both regular and random waves, least reflection from the circular curve bottom profile, less pressures on the seaside of the lip wall has resulted in higher efficiency.

5.5. Wave amplification inside the chamber

The wave amplification factor for regular waves, β_{reg} and for random waves, β_{ran} based on the Eqns. (14) and (15) are projected in Figs. 13 and 14 respectively. It is well known that the efficiency of an OWC system is controlled by the magnitude of oscillation of air column driven by the oscillations of the water surface within the chamber. It is seen that the trend in the variation of β_{reg} with d/L for all the models is similar. The effect of d/L on β_{reg} is found pronounced for d/L < 0.14, beyond which the effect is found to be

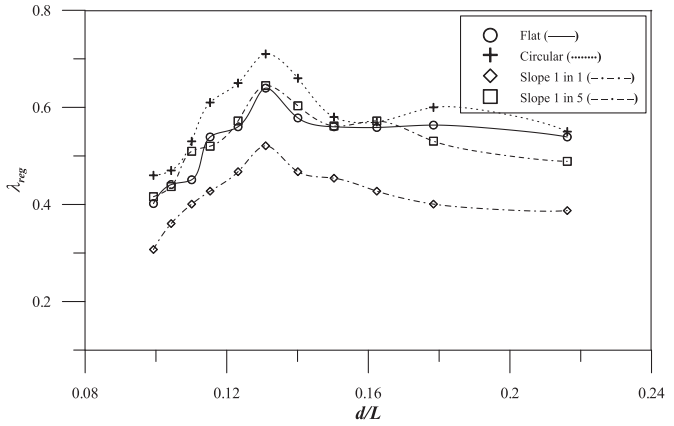

Fig. 7. Hydrodynamic efficiency (λ_{reg}) of OWC corresponds to the relative water depth. (Regular waves) (H/L from 0.0122 to 0.0194).

insignificant. Further, the results demonstrate that β_{reg} is the highest for the OWC with circular bottom. As stated earlier that $(p_{fout})_{max}/\rho gH$ being higher for the models with bottom slope of 1:1 and flat, β_{reg} is found to be lower due to immediate obstruction to the fluid flow causing a radiated flow inside the chamber and the vortices formation in the vicinity of the lip wall reduces the free surface oscillation of water. Among the other, two bottom profiles, one with bottom slope 1:5 and circular curve, the latter has the capability of larger fluid particle entrance length and low obstruction to the waves leading to an increase in water surface oscillation inside the chamber. Higher the wave amplification leads to the higher volume of air compression, which will eventually yield high output power. The variation of β_{ran} with d/L_p is found similar to that observed for the regular wave tests.

5.6. Wave power absorption coefficient

The flow direction occurs from high to low pressure region; the wave power absorption (WPA) coefficient also working on this same principle. Due to the differences in pressure amid the inner and outer chamber walls (low pressure at the inside of the chamber and high fluid pressure seaside of the lip wall), the flow takes place towards the inside of the chamber. According to the principle of OWC, the fluid pressure near the chamber mouth can have two components namely active component and reactive component as discussed by Falnes [3]. The active component is responsible for flow oscillation inside the chamber, while, the reactive component causing wave amplification near the mouth.

The WPA_{reg}, due to regular waves and due to random waves, WPA_{ran} as a function to the corresponding relative water depths for the four models are presented in Figs. 15 and 16 respectively. It is observed that at natural frequency, i.e., $d/L = 0.131$ (for regular) and $d/L_p = 0.1223$ (for random), the OWC models with flat bottom as well as with curve exhibits a higher WPA further observed that $d/L > 0.14$ and d/L_p between 0.09 and 0.13 WPA coefficient measured with minimal oscillation. This is due to the fact that it depends on both β and p_{fout}. The slope 1:1 bottom profile shows the least WPA due to higher reflection and immediate obstruction to the flow passage enter in to the chamber of OWC. The results are found to be similar for the random wave tests.

5.7. Air pressure ratio to the incident pressure

The air pressure ratio, representing the air pressure changes inside the OWC air chamber due to rise and fall of water for regular

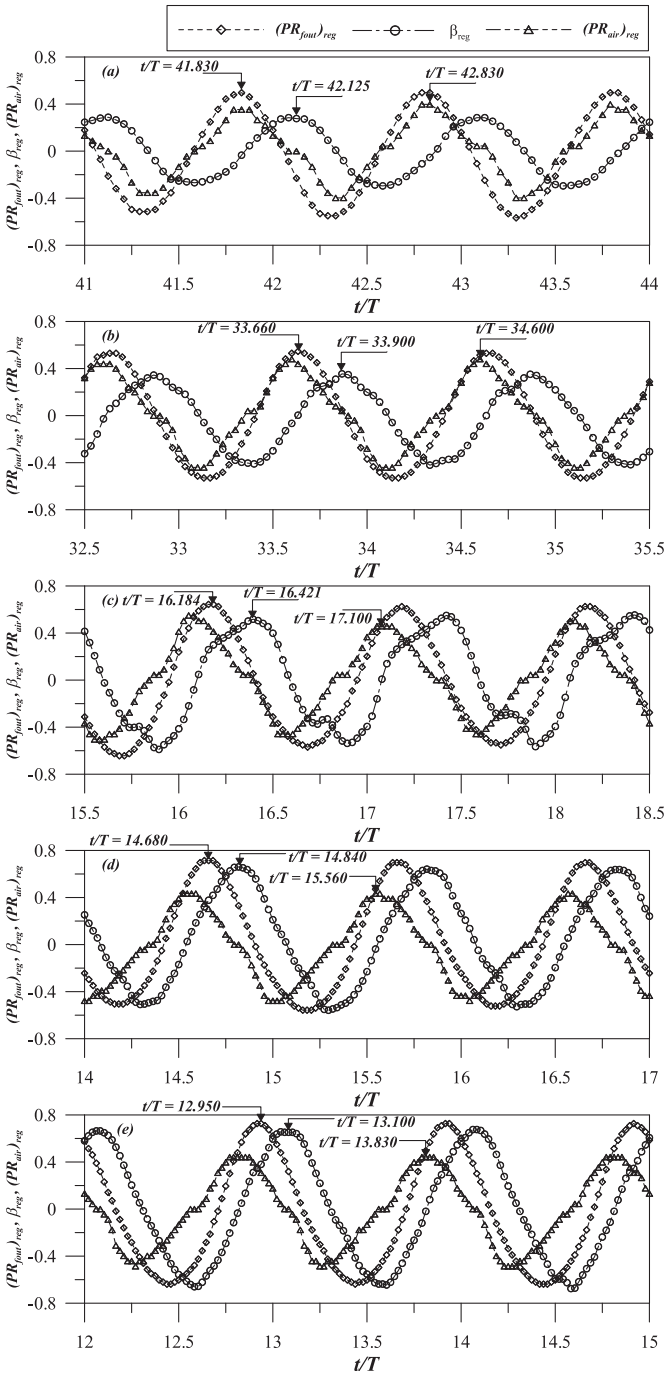

Fig. 8. Comparison of time series in quantifying phase difference between $(PR_{fout})_{reg}$, β_{reg} and $(PR_{air})_{reg}$ against t/T. (a) d/L = 0.244 & H/L = 0.0276, (b) d/L = 0.178 & H/L = 0.0221, (c) d/L = 0.131 & H/L = 0.0141, (d) d/L = 0.110 & H/L = 0.0126, (e) d/L = 0.099 & H/L = 0.0111 (Circular curve bottom profile).

Table 1
Quantitative phase difference between $(PR_{fout})_{reg}$, β_{reg}, $(PR_{air})_{reg}$ in terms of t/T for different relative water depth at constant wave height (Circular curve bottom profile).

d/L	$(PR_{fout})_{reg}$ (t/T)	β_{reg} (t/T)	$(PR_{air})_{reg}$ (t/T)	β_{reg} (t/T) − $(PR_{air})_{reg}$ (t/T)
0.244	41.830	42.125	42.830	−0.705
0.178	33.660	33.900	34.600	−0.700
0.131	16.184	16.421	17.100	−0.679
0.110	14.680	14.840	15.560	−0.720
0.099	12.950	13.100	13.830	−0.730

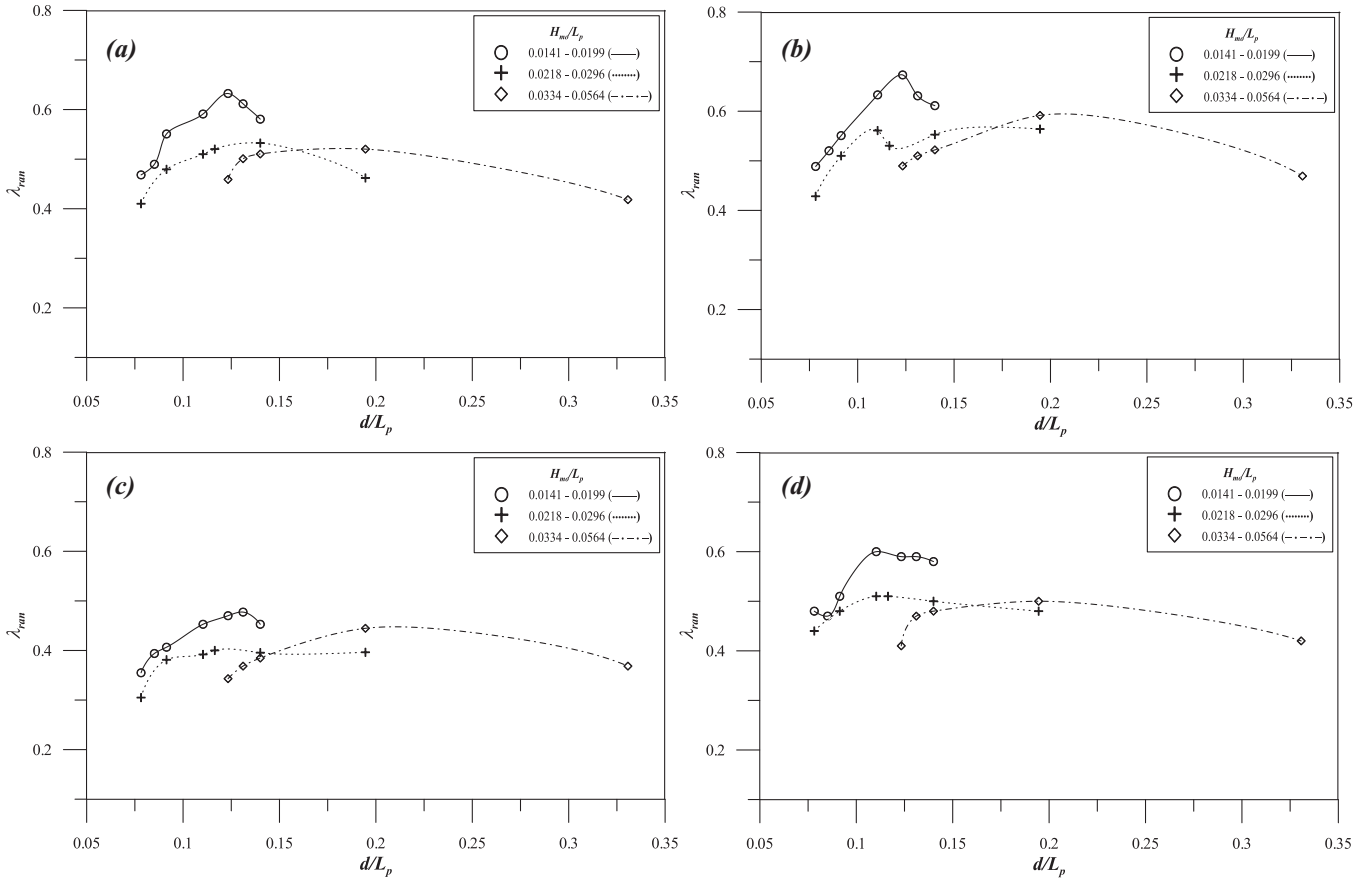

Fig. 9. a Hydrodynamic efficiency (λ_{ran}) of flat bottom OWC corresponds to the relative water depth. (Random waves). b Hydrodynamic efficiency (λ_{ran}) of circular curve bottom OWC corresponds to the relative water depth. (Random waves). c Hydrodynamic efficiency (λ_{ran}) of slope 1 in 1 bottom OWC corresponds to the relative water depth. (Random waves). d Hydrodynamic efficiency (λ_{ran}) of slope 1 in 5 bottom OWC corresponds to the relative water depth. (Random waves).

waves, $(PR_{air})_{reg}$ and for random waves, $(PR_{air})_{ran}$ based on the Eqns. (12) and (13) as a function of their corresponding d/L are depicted in Figs. 17 and 18 respectively. The results indicate that the oscillation in its variation for the model with bottom curve is minimum, thus indicating that the flow of energy will be smooth, thus posing minimum problems to the smooth running of the turbine. In the case of random wave results a reduction in air pressure by about 15–20%, as it is due to the averaging of a number components involved in the description of the wave climate. One interesting phenomena to be noted is that in both the regular and random wave results, the outcome of air pressure over the range of d/L tested is not found significant in its oscillation. This is an important requirement for the mechanical efficiency of the OWC system to be more efficient. The trend in the variation of all the parameters for the four bottom profile OWC models have exhibited similar trend in their variation revealing that the natural period for the models

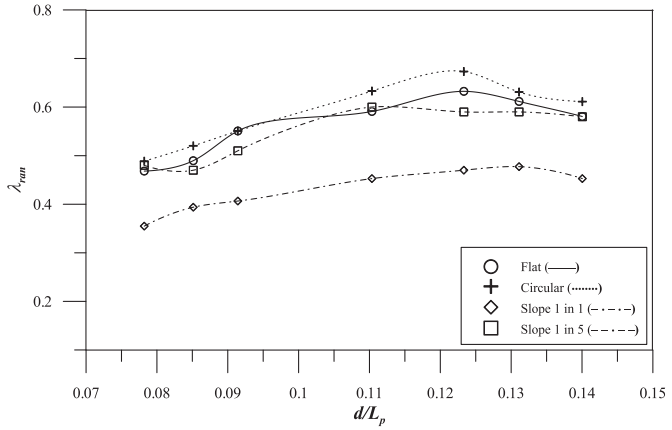

Fig. 10. Hydrodynamic efficiency (λ_{ran}) of OWC corresponds to the relative water depth. (Random waves) (H_{m0}/L_p from 0.0141 to 0.0199).

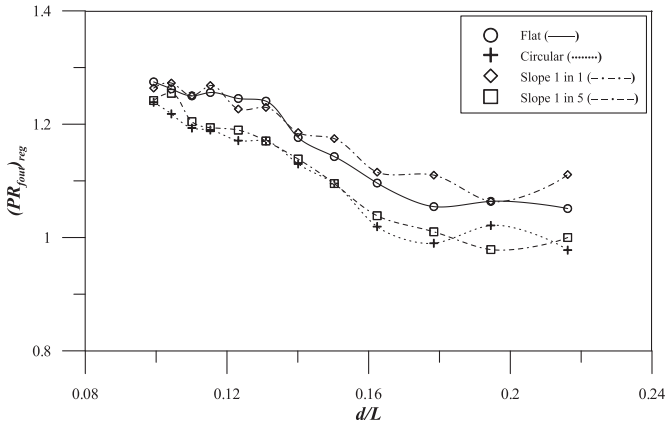

Fig. 11. Pressure ratio corresponds to fluid pressure at the mouth. (Regular waves) (H/L from 0.0122 to 0.0194).

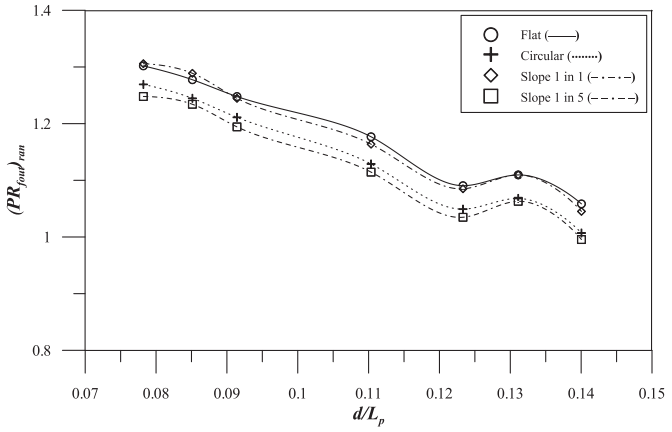

Fig. 12. Pressure ratio corresponds to fluid pressure at the mouth. (Random waves) (H_{m0}/L_p from 0.0141 to 0.0199).

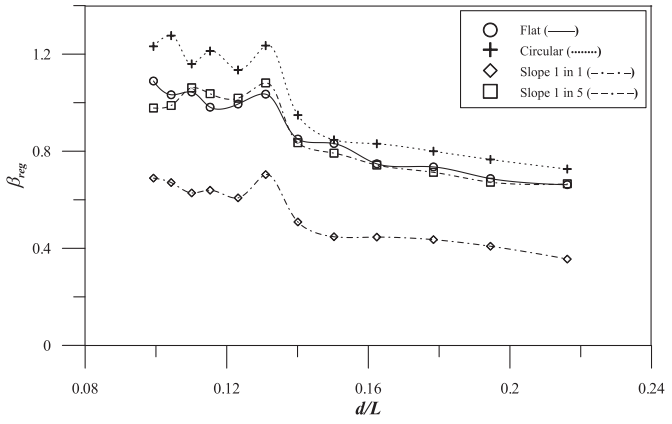

Fig. 13. Wave amplification factor (β_{reg}) corresponds to the relative water depth. (Regular waves) (H/L from 0.0122 to 0.0194).

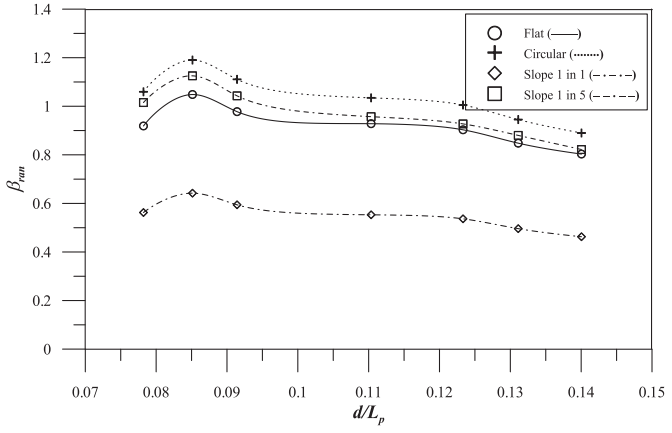

Fig. 14. Wave amplification factor (β_{ran}) corresponds to the relative water depth. (Random waves) (H_{m0}/L_p from 0.0141 to 0.0199).

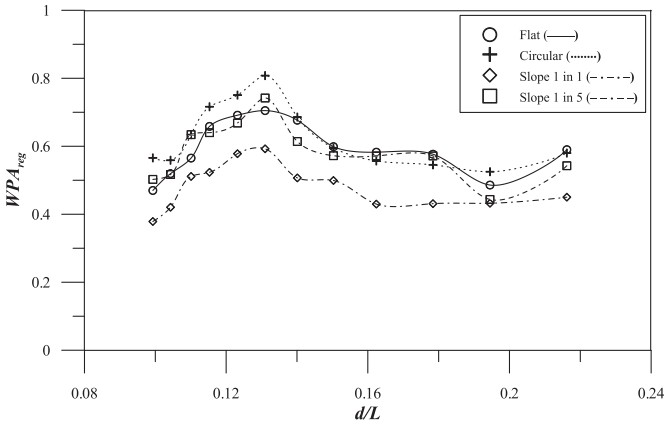

Fig. 15. Wave power absorption coefficient of OWC corresponds to the relative water depth. (Regular waves) (H/L from 0.0122 to 0.0194).

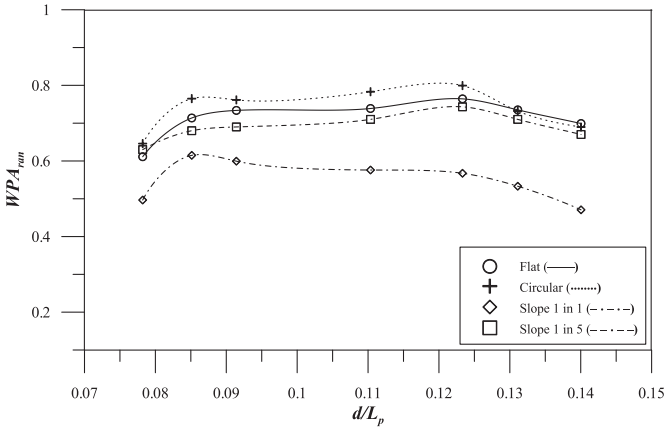

Fig. 16. Wave power absorption coefficient of OWC corresponds to the relative water depth. (Random waves) (H_{m0}/L_p from 0.0141 to 0.0199).

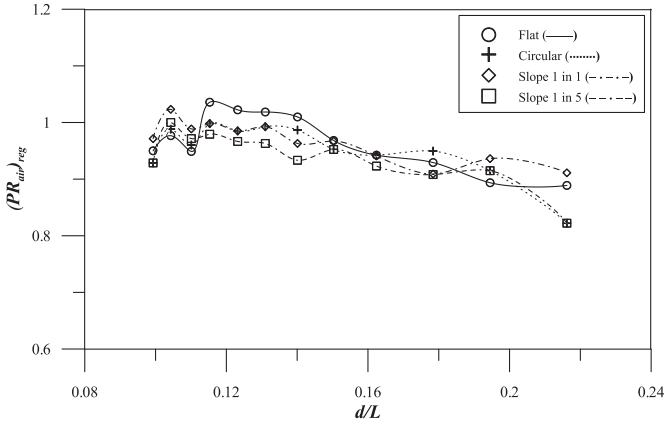

Fig. 17. Pressure ratio corresponds to fluid pressure at top plate of the chamber. (Regular waves) (H/L from 0.0122 to 0.0194).

tested is same. This is mainly because of the trend dictating phase difference between different hydrodynamic parameters for the four profiles observed to be same. The time series quantifying phase difference of four different configurations against t/T for different hydrodynamic parameters $(PR_{fout})_{reg}$, β_{reg}, $(PR_{air})_{reg}$ corresponds to d/L of 0.244 and 0.131 are shown in Figs. 19 and 20.

5.8. Reflection nature of OWC models

The degree of wave reflection is defined by the reflection coefficient $k_r = H_r/H_i$, where, H_r and H_i are the reflected and incident wave heights, respectively. Two number of resistance type wave probes, one at 5 m, $\eta_2(t)$ and 5.31 m, $\eta_3(t)$ from the model, inside each of the four longitudinal sections, were used to measure the composite wave elevation, which later was used to decompose into incident and reflected components as per the method of Goda and Suzuki [5] is used to determine the reflection coefficient, for all the models under regular and random waves. The reflection coefficient, $k_{r\,(reg)}$ for regular and $k_{r\,(ran)}$ for random waves as a function of their corresponding relative water depths for the four models are depicted in Figs. 21 and 22 respectively. It is inferred from the results that in general, $k_{r\,(reg)}$ are highest for the model with bottom profile slope 1 in 1, followed by the models with flat, slope 1 in 5 and circular bottom profiles. The $k_{r\,(reg)}$ near the natural period of the system is found to be a minimum leading to maximum efficiency. The smooth entrance offered by circular and 1 in 5 slope decreases the reflection from the OWC. The reflection coefficient is high at high frequency because of minimum wave power absorption i.e., most of the energy is reflected back. At $d/L = 0.131$ and $d/L_p = 0.1223$, there is a reduction in reflected energy due to higher wave absorption, causing maximum efficiency. Further in low frequency the trend is slightly increasing compared to high frequency waves since longer waves have high reflection coefficient compared to shorter waves due to OWC absorbing wave energy from all the low frequency waves. Similar type of trend is seen for random waves with less reflection coefficient at natural frequency of the system and increases towards low frequency zone. From the point of less magnitude of reflection coefficient, OWC with its bottom profile formed by a circular curve would be preferred.

6. Conclusions

The performance characteristics of OWC models with four different bottom slopes in regular and random wave fields have been assessed through a well-controlled comprehensive experimental program. The following are the conclusions drawn from the study.

1. The investigation of air hole ratio, a/A varied from 0.1% to 1.2% of plan area of the chamber, on the efficiency of the OWC has proved that a value between 0.6% and 0.7% is optimum with which a maximum efficiency of about 0.64 is achieved. The value of a/A as 0.68% is adopted for all the tests reported in this study.
2. The OWC with circular curve bottom profile has been proved to have a better efficiency than the other three shapes because of higher wave amplification, higher air pressure ratio, higher wave absorption coefficient and less reflection.

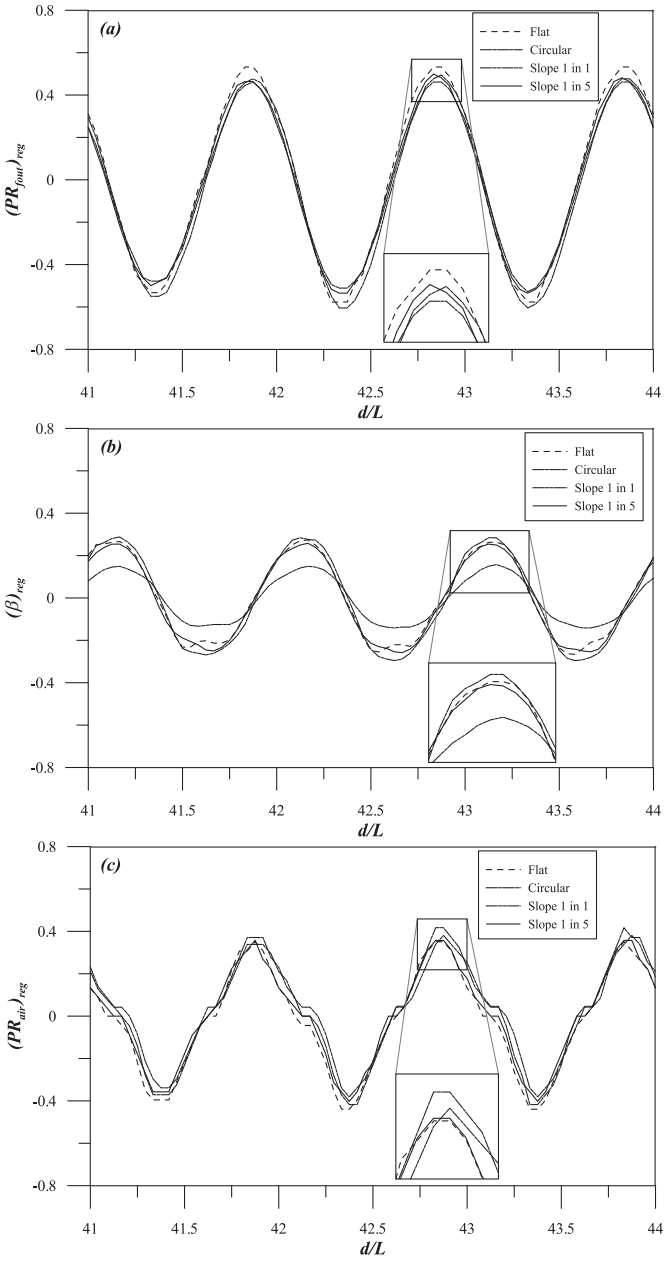

Fig. 19. Comparison of time series in quantifying phase difference for four different bottom profiles against t/T (a) $(PR_{fout})_{reg}$, (b) β_{reg} and (c) $(PR_{air})_{reg}$ ($d/L = 0.244$ and $H/L = 0.0276$).

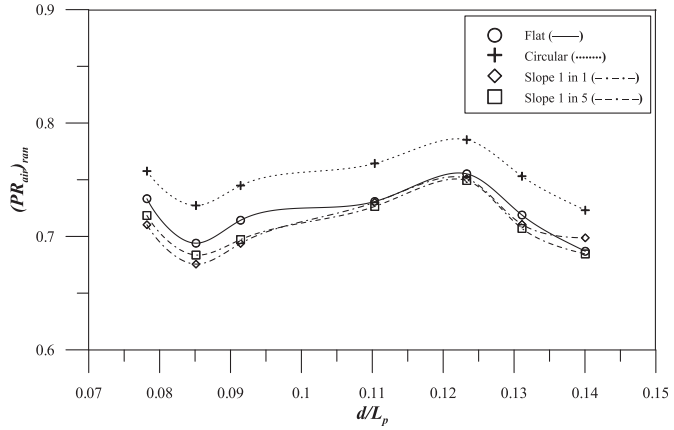

Fig. 18. Pressure ratio corresponds to fluid pressure at top plate of the chamber. (Random waves) (H_{m0}/L_p from 0.0141 to 0.0199).

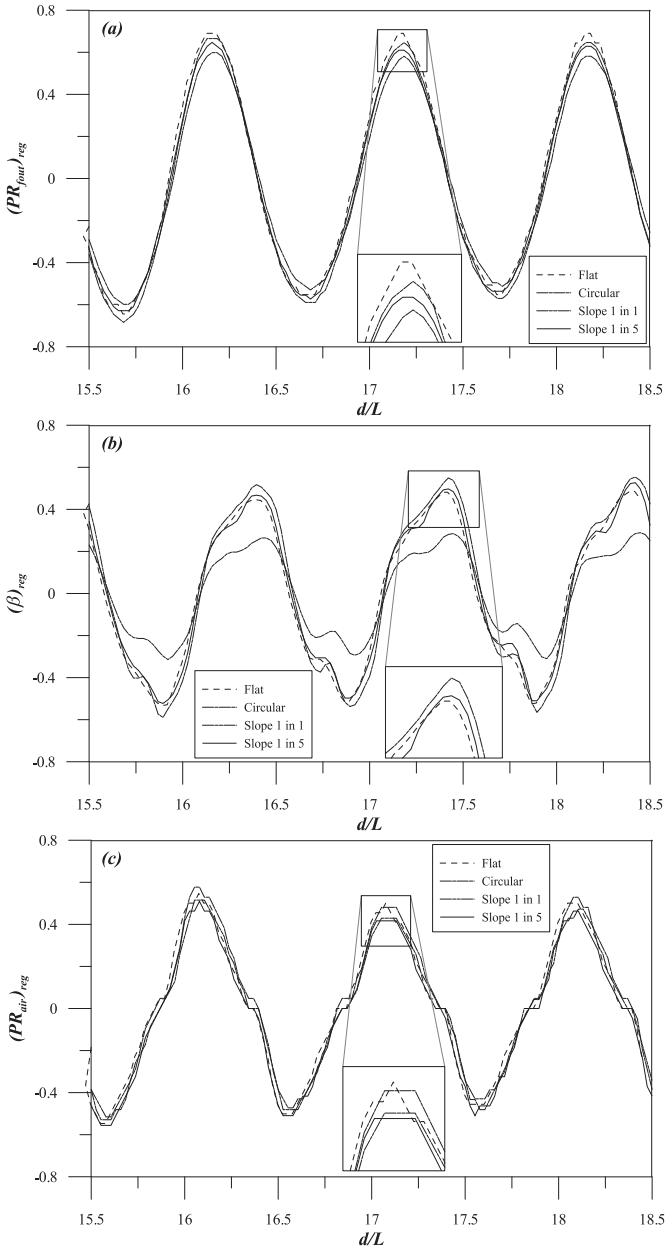

Fig. 20. Comparison of time series in quantifying phase difference for four different bottom profiles against t/T (a) $(PR_{fout})_{reg}$, (b) β_{reg} and (c) $(PR_{air})_{reg}$ (d/L = 0.131 and H/L = 0.0141).

3. In general, the efficiency increases with an increase in d/L, attaining a maximum at d/L = 0.131 and $d/L_p = 0.1223$, (where L and L_p are corresponds to the natural frequency of the system) due to higher fluid flow length.
4. The efficiency decreases with an increase in wave steepness, due to higher reflection from the lip wall and also with the shape of the bottom profile of the OWC.
5. The natural frequency of the system was observed to be unaltered for different bottom profile configurations.
6. Lesser front wall outside pressure, higher wave absorption, minimum reflection for the circular curve and slope 1 in 5 bottom profile OWC results in a higher wave amplification inside the chamber.
7. Even though the magnitude of air pressure ratio is of similar order for all the bottom profile configurations, the OWC with circular curve bottom profile yields higher air pressure ratio for the random wave incidences.

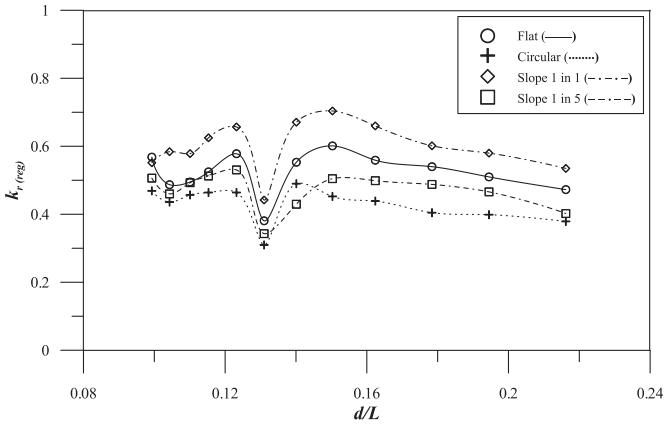

Fig. 21. Reflection coefficient $k_{r\ (reg)}$ of OWC corresponds to the relative water depth. (Regular waves) (H/L from 0.0122 to 0.0194).

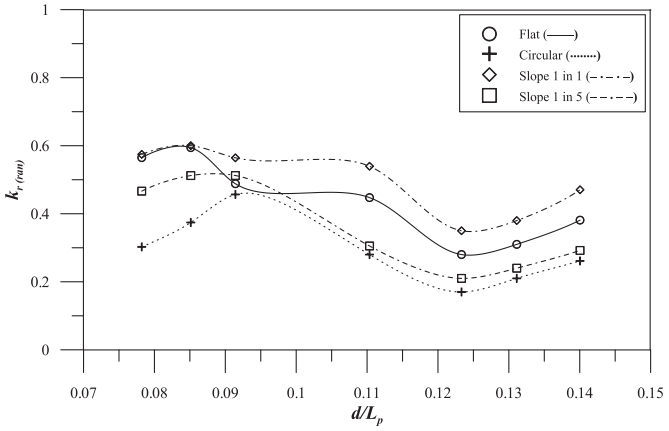

Fig. 22. Reflection coefficient $k_{r\ (ran)}$ of OWC corresponds to the relative water depth. (Random waves) (H_{m0}/L_p from 0.0141 to 0.0199).

Acknowledgement

This research was funded by Norwegian Research Council (Grant No. 217622/E20) and their support is gratefully acknowledged.

References

[1] J.M.B.P. Cruz, A.J.N.A. Sarmento, Energia das Ondas: Introdução aos Aspectos Tecnológicos, Econômicos e Ambientais, Instituto do Ambiente, Amadora, 2004 in Portuguese.
[2] D.V. Evans, R. Porter, Hydrodynamic characteristics of an oscillating water column device, Appl. Ocean Res. 18 (1995) 155–164.
[3] J. Falnes, Ocean Waves and Oscillating Systems, Cambridge University Press, 2005. ISBN 1139431935.
[4] M. Folley, T.J.T. Whittaker, Analysis of the nearshore wave energy resource, Renew. Energy 34 (7) (2009) 1709–1715.
[5] Y. Goda, Y. Suzuki, Estimation of incident and reflected waves in random wave experiments, in: 15th Coastal Engineering Conference, Hawaii, 1976.
[6] I. López, B. Pereiras, F. Castro, G. Iglesias, Performance of OWC wave energy converters: influence of turbine damping and tidal variability, Int. J. Energy Res. 39 (4) (2015) 472–483.
[7] O. Malmo, A. Reitan, Wave-power absorption by an oscillating water column in a channel, J. Fluid Mech. 158 (1985) 153–175.
[8] M.E. McCormick, Ocean Energy Conversion, John Wiley & Sons, 1981.
[9] P. McIver, D.V. Evans, An approximate theory for the performance of a number of wave energy devices set into a reflecting wall, Appl. Ocean Res. 10 (2) (1988) 58–65.
[10] M. Ravindran, P.M. Koola, Energy from sea waves—the Indian wave energy

program, Curr. Sci. 60 (1991) 676–680.
[11] K. Rezanejad, J. Bhattacharjee, C. Guedes Soares, Stepped sea bottom effects on the efficiency of nearshore oscillating water column device, Ocean Eng. 70 (2013) 25–38.
[12] D. Ross, Power from Sea Waves, Oxford University Press, 1995.
[13] V. Sundar, M. Torgeir, H. Jorgen, Conceptual designs on integration of oscillating water column devices in breakwaters, in: Proc. of the ASME 29th Intl. Conf. on Ocean, Offshore and Arctic Eng, Shanghai, 2010. June 6–11, pp. 479–489.
[14] R. Shaw, Wave Energy: a Design Challenge, Ellis Horwood, Chichester, 1982.
[15] K. Thiruvenkatasamy, S. Neelamani, On the efficiency of wave energy caisson in array, Appl. Ocean Res. 19 (1997) 61–72.
[16] M.T.M. Thomas, R.J. Irvin, K.P. Thiagarajan, Investigation into the hydrodynamic efficiency of an oscillating water column, J. Offshore Mech. Arct. Eng. 129 (2007) 273–280.
[17] Ruo-Shan Tseng, Rui-Hsiang Wu, Chai-Cheng Huang, Model study of a shoreline wave-power system, Ocean Eng.. 27 (2000) 801–882.
[18] D.J. Wang, M. Katory, Y.S. Li, Analytical and experimental investigation on the hydrodynamic performance of onshore wave-power devices, Ocean Eng. 29 (2002) 871–885.
[19] T.J.T. Whittaker, S.J. McIlwaine, S. Raghunathan, A review of the Islay shoreline wave power station, in: Proceedings of First European Wave Energy Symposium, 1993, pp. 283–286.
[20] R. Wilbert, Hydrodynamic Characteristics of Double Chamber Oscillating Water Column Device, Doctoral thesis, Indian Institute of Technology Madras, India, 2013, pp. 137–138.
[21] Y. Zhang, Q.P. Zou, D. Greaves, Air-water two phase flow modelling of hydrodynamic performance of an oscillating water column device, Renew. Energy 41 (2012) 159–170.
[22] W. Zheng, Experimental research and parameters optimization of a prototype OWC wave power device, in: Proc. International Conference on Ocean Energy Recovery, 1989, pp. 43–50.